

Reconstructing Current Distributions from Biomagnetic Measurements Under Large External Noise Disturbances

Kensuke Sekihara, *Member, IEEE*, Bernhard Scholz, Herbert Bruder, and Rainer Graumann

Abstract—External noise fields cause spatially coherent noise in the biomagnetic data measured by a multichannel magnetometer. This paper proposes a method of incorporating this spatial coherence into current-density reconstruction. This method can reconstruct current distributions from biomagnetic measurements affected by external noise fields. Computer simulations demonstrate its effectiveness.

I. INTRODUCTION

NEURON ACTIVITIES in the human brain induce bioelectric current, which generates weak magnetic fields that can be detected by a SQUID (Super Conducting Quantum Interference Device) magnetometer on the scalp surface [1]. The aim of biomagnetic imaging is to visualize those activities by reconstructing the biocurrent distributions from a measured magnetic field. One of the problems here is to develop an efficient algorithm for reconstructing such biocurrent distributions.

Two approaches have been investigated to solve this problem. One approach introduces an equivalent current dipole (ECD) [1] with which the biocurrent distributions can be modelled. The concepts behind the ECD are physiologically plausible to some extent, and some biomagnetic data can be explained by the existence of a single ECD. However, when a bioelectric current distribution pattern is so complex that it must be modelled by multiple ECD's, the estimation of such biocurrent distributions becomes highly nonlinear [2], and no method is currently available to effectively solve this nonlinear optimization problem.

The other approach assumes voxels in the region of interest, and tries to reconstruct the biocurrent distribution assigned to those voxels without imposing any models on the distribution. This approach is similar to the image reconstruction used in various kinds of medical imaging apparatuses. One well-known [3] [4] algorithm belonging to this approach uses the pseudo inversion of the lead field matrix that expresses the sensitivity of detector coils at voxel locations. Although this algorithm has been successfully applied to actually measured neuromagnetic data [5], it still has several problems.

Manuscript received December 7, 1992; revised May, 5, 1993. The associate editor responsible for coordinating the review of this paper and recommending its publication was E. Stokely.

K. Sekihara is with the Central Research Laboratory, Hitachi, Ltd., Tokyo 185, Japan.

B. Scholz, H. Bruder, and R. Graumann are with Siemens AG, Medical Engineering Group, 8520 Erlangen, Germany.

IEEE Log Number 9215300D.

One such problem is that the algorithm sometimes fails to reconstruct the correct current distribution when the signal-to-noise ratio of the measurement is low. The measurements of the biomagnetic field from a human brain often suffer from a very low signal-to-noise ratio. In many cases, this is primarily due to the external noise magnetic fields in the measurement environment, rather than the noise caused by the SQUIDs or the electronics associated with them. Recently, Knuutila et al. [6] and also Sekihara et al. [7] have proposed to utilize the spatial coherence of external noise to remove its influence when estimating the parameters of an ECD.

This paper extends this previously proposed method [7], and proposes a novel algorithm for reconstructing biocurrent distributions under large external noise disturbances. The algorithm can remove the influence of external noise disturbances by incorporating their spatial coherence. In this paper, Section 2 describes the proposed reconstruction. In Section 3, the algorithm's effectiveness is demonstrated by computer simulation, where the measurements of an evoked neuromagnetic field are simulated.

In that computer simulation, we assume the existence of not only an environmental external noise field caused by randomly fluctuating magnetic dipoles but also the noise field caused by a randomly rotating current dipole existing in a brain. This latter noise simulates a noise field caused by spontaneous brain activity, which is often referred to as brain noise. A magnetically shielded room, a higher order gradiometer, and other noise reduction methods using additional reference detectors [8] cannot effectively remove the influence of brain noise, because the distances between the noise source and the detector coils are often comparable to those between a signal source and the coils. The computer simulation clearly demonstrates that the proposed method can successfully eliminate the influence of such brain noise.

II. METHOD

Let us define the component of the magnetic field measured at the m th detector coil as B_m and a set of measured data as a vector $\mathbf{B} = (B_1, B_2, \dots, B_M)^T$. Here, M is the total number of detector coils and the superscript T indicates the matrix transpose. Let us also define the unknown primary current [9] distribution as a vector $\mathbf{f} = (f_1, f_2, \dots, f_{3N})^T$ where N is the total number of voxels. The x , y , and z components of the primary current at the n th voxel are

assigned to $f_{3(n-1)+1}$, $f_{3(n-1)+2}$, and $f_{3(n-1)+3}$, respectively. The relationship between the two vectors \mathbf{B} and \mathbf{f} is linear and is expressed as $\mathbf{B} = L\mathbf{f}$. Here, L is an $M \times (3N)$ matrix and its elements, $L_{m,3(n-1)+1}$, $L_{m,3(n-1)+2}$, and $L_{m,3(n-1)+3}$, represent the sensitivity of the m th detector to the x , y , and z components of the primary current at the n th voxel. This matrix L is called the lead field matrix.

In conventional reconstruction, current estimates $\hat{\mathbf{f}}$ are obtained by minimizing the cost function $E = \|\mathbf{B} - \hat{\mathbf{B}}\|^2$, where $\hat{\mathbf{B}} = L\hat{\mathbf{f}}$. This minimization has a well-known solution using the Moore-Penrose generalized inverse [10]. Namely, for $M < 3N$,

$$\hat{\mathbf{f}} = L^T(LL^T)^{-1}\mathbf{B}. \quad (1)$$

In practice, to avoid the numerical instability associated with the matrix inversion, matrix regularization is often used, and, in such cases, the current estimates $\hat{\mathbf{f}}$ are calculated from [11]

$$\hat{\mathbf{f}} = L^T(LL^T + \gamma I)^{-1}\mathbf{B} \quad (2)$$

where I is the unit matrix and γ is the predetermined regularization parameter. Note that the estimates calculated using (2) minimize the cost function [12]

$$E = \|\mathbf{B} - \hat{\mathbf{B}}\|^2 + \gamma\|\hat{\mathbf{f}}\|^2. \quad (3)$$

Consequently, the estimates obtained using (2) provide a compromise solution between the minimization of the current norm $\|\hat{\mathbf{f}}\|^2$ and the norm of the squared error term, $\|\mathbf{B} - \hat{\mathbf{B}}\|^2$.

When a multichannel magnetometer that can simultaneously measure the magnetic field data is used, the external noise fields cause spatially correlated noise in the measured data. This is because simultaneous measurement preserves the spatial coherence of such external noise. Consequently, if this correlation can be taken into account when reconstructing current distributions, the influence of the external noise fields can be reduced in the reconstruction.

According to the maximum likelihood principle, when the noise is spatially correlated and when the noise can be considered to be multivariate Gaussian noise, the squared error term can be expressed as $(\mathbf{B} - \hat{\mathbf{B}})^T C^{-1} (\mathbf{B} - \hat{\mathbf{B}})$, instead of $\|\mathbf{B} - \hat{\mathbf{B}}\|^2$ [7]. Here, C is the noise covariance matrix that expresses the spatial correlation of the noise in the measured data. Thus, in the proposed reconstruction, the minimum norm current estimates are calculated by minimizing the cost function,

$$E = (\mathbf{B} - \hat{\mathbf{B}})^T C^{-1} (\mathbf{B} - \hat{\mathbf{B}}) + \gamma\|\hat{\mathbf{f}}\|^2. \quad (4)$$

Here, the noise covariance matrix C should be obtained in advance of the reconstruction. The solution to this minimization is known to be [13]

$$\hat{\mathbf{f}} = (L^T C^{-1})(LL^T C^{-1} + \gamma I)^{-1}\mathbf{B}. \quad (5)$$

This equation should be used to reconstruct biocurrent distributions with reduced external noise influence. Here, the regularization parameter γ can be chosen such that the term $(\mathbf{B} - \hat{\mathbf{B}})^T C^{-1} (\mathbf{B} - \hat{\mathbf{B}})$ is equal to M , the average value of the χ^2 statistics. Here, note that the term $(\mathbf{B} - \hat{\mathbf{B}})^T C^{-1} (\mathbf{B} - \hat{\mathbf{B}})$ is known to obey the χ^2 statistics if the measured data contain

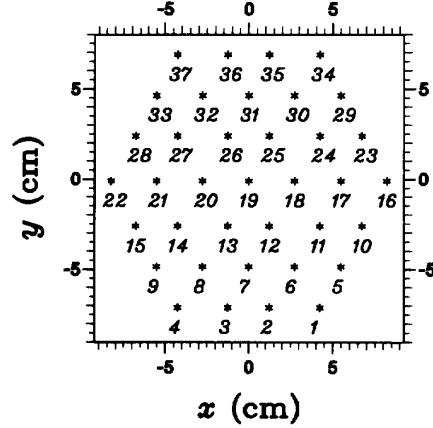


Fig. 1. Alignment of detector coils. The asterisks * indicate each coil's location, and the figure written under each asterisk is the number for that channel.

multivariate Gaussian noise. This criterion has been frequently used in maximum entropy image reconstruction [14].

To calculate noise covariance matrix C , one should set, in the measured data, a time window where the data contain only noise fields and do not contain any signal fields. Here, we assume that the ensemble average of the external noise can be replaced with its time average, namely the external noise is ergodic. Let us define the data measured by the m th detector channel within such a time window as $\Gamma_m(t)$, where $m = 1, 2, \dots, M$. Then, the element (i, j) of the covariance matrix C_{ij} is calculated from

$$C_{ij} = \langle \Gamma_i(t) - \langle \Gamma_i(t) \rangle \rangle \langle \Gamma_j(t) - \langle \Gamma_j(t) \rangle \rangle \quad (6)$$

where $i, j = 1, 2, \dots, M$ and the bracket $\langle \rangle$ indicates the average over the time window.

III. COMPUTER SIMULATIONS

A. General Description

Computer simulations are performed to verify the effectiveness of the method proposed in the preceding section. The reconstruction of a biocurrent distribution that generates an evoked neuromagnetic field is simulated. The general features of this computer simulation are as follows.

A magnetometer with 37 channels, each having a first-order gradiometer coil with a 7.1-cm baseline, is assumed to be used for measuring the evoked field. The gradiometer coils are hexagonally aligned on a plane defined as the x - y plane with its origin equal to the center of this hexagon. The detector coil alignment is shown in Fig. 1. The z direction is defined as the direction perpendicular to this detector-aligned-plane. The values of the spatial coordinates (x, y, z) are expressed in centimeters. The unit of time appearing in Section 3 is always seconds, unless otherwise noted.

In this computer simulation, the spherically symmetric homogeneous conductor model is assumed, and the magnetic field created by an ECD at each detector coil location \mathbf{r} is

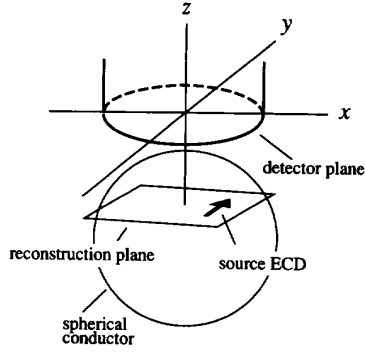


Fig. 2. Geometry and coordinate system used for the computer simulation.

calculated using the equation shown below [9]

$$\mathbf{B}(\mathbf{r}) = \frac{\mu_0}{4\pi\Phi^2} (\Phi(\mathbf{Q} \times \mathbf{r}_0) - (\mathbf{Q} \times \mathbf{r}_0 \cdot \mathbf{r}) \nabla \Phi) \quad (7)$$

where $\Phi = |\mathbf{a}|(|\mathbf{r}||\mathbf{a}| + |\mathbf{r}|^2 - \mathbf{r}_0 \cdot \mathbf{r})$ and $\mathbf{a} = \mathbf{r} - \mathbf{r}_0$. The vectors \mathbf{r}_0 and \mathbf{Q} indicate the position and the moment of the ECD. In this equation, the position vectors \mathbf{r} and \mathbf{r}_0 have origins equal to the center of the sphere. Note that (7) takes the volume current effects into account, and that the magnetic field outside the spherical volume conductor does not depend on its conductivity or its radius. The center of the sphere is assumed to be located at $(0, 0, -15)$. The magnetic field data are obtained by subtracting the field strength at the gradiometer's upper coil position from that at the lower coil position. These simulated time data are generated using a 10-ms sampling period (100 Hz sampling frequency) for a time interval of $-2 \leq t_k \leq 1$. Here, the time at which data are sampled is denoted by t_k and the total number of sample points contained in $-2 \leq t_k \leq 1$ is denoted by K . In this computer simulation, K is equal to 300.

Since each element of the lead field matrix is calculated by using (7), only the primary current sources are reconstructed in this computer simulation. Here, the x - y plane containing the simulated evoked neural current is assumed to be known in advance, and the current density distribution in this plane is reconstructed. The reconstruction region covers $-8 \leq x \leq 8$ and $-8 \leq y \leq 8$ and consists of 17×17 pixels. The geometry of the computer simulation is shown in Fig. 2. In the reconstruction, the regularization parameter γ can be chosen such that the term $(\mathbf{B} - \hat{\mathbf{B}})^T \mathbf{C}^{-1} (\mathbf{B} - \hat{\mathbf{B}})$ is equal to M , as mentioned in the preceding section. Here, γ is set at $6.0 \times 10^{-3} \lambda_{\max}$, where λ_{\max} is the largest eigenvalue of the matrix $\mathbf{L}\mathbf{L}^T$ when using (2) or that of $\mathbf{L}\mathbf{L}^T \mathbf{C}^{-1}$ when using (5). That value gives $(\mathbf{B} - \hat{\mathbf{B}})^T \mathbf{C}^{-1} (\mathbf{B} - \hat{\mathbf{B}}) \simeq M$ in this computer simulation.

B. Generation of Simulated Evoked Field

A single ECD assumed to exist at the fixed location $(3, 0, -4)$ is used as the model of the evoked neural current source. This dipole is assumed to make a single 80-ms long rotation in the x - y plane after a stimulus is applied. Thus, by defining the time instant when a stimulus is applied as

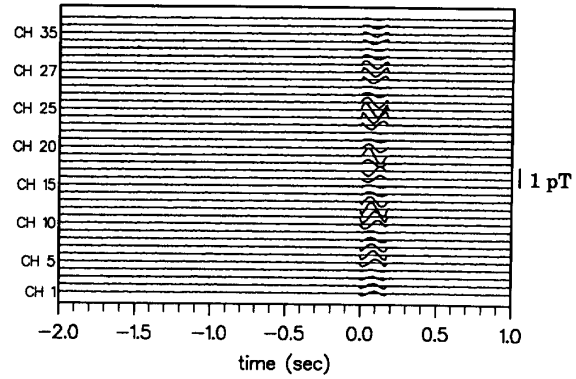


Fig. 3. Thirty-seven channel recordings of the simulated evoked neuromagnetic field $S_m(t_k)$. The stimulus is applied at $t = 0$ sec. The data are calculated assuming that a single ECD located at $(3, 0, -4)$ makes an 80-ms long rotation in the x - y plane after a stimulus is applied.

$t = 0$, the dipole moment of this ECD, $\mathbf{d} = (d_x, d_y, d_z)$, can be expressed as

$$\begin{aligned} d_x &= |\mathbf{d}| \cos(2\pi t_k / \tau_1), & d_y &= |\mathbf{d}| \sin(2\pi t_k / \tau_1) \\ d_z &= 0 & \text{for } t_k \geq 0 \end{aligned}$$

and

$$\mathbf{d} = 0, \quad \text{for } t_k < 0 \quad \text{and} \quad t_k > \tau_1.$$

Here, τ_1 is a time constant equal to 80 ms. The intensity of the moment $|\mathbf{d}|$ is set at $0.02 \text{ mA} \cdot \text{mm}$. The magnetic field data are calculated by subtracting the gradiometer's upper coil output from the lower coil output.

Next, the noise intrinsic to each detector channel is calculated using a Gaussian random number generator. This intrinsic noise represents the noise from SQUIDS and their associated electronics. The standard deviation of the intrinsic noise is set at 0.01 pT for all channels. The simulated evoked field data are calculated by adding the intrinsic Gaussian noise to the magnetic field data. The m th detector channel recordings of this simulated evoked field at time t_k are defined as $S_m(t_k)$. This $S_m(t_k)$ for $-2 \leq t_k \leq 1$ is shown in Fig. 3.

Two time instants, $t_e = 20 \text{ ms}$ and $t_f = 60 \text{ ms}$, are chosen and two data sets, $S_m(t_e)$ and $S_m(t_f)$, are used to reconstruct the simulated neural current. Note that the moment of the source dipole is $(0, 0.02, 0)$ at t_e and $(0, -0.02, 0)$ at t_f . The average intensities of the signal field at t_e and t_f , $\sqrt{\frac{1}{M} \sum_{m=1}^M S_m^2(t_e)}$ and $\sqrt{\frac{1}{M} \sum_{m=1}^M S_m^2(t_f)}$, are both equal to 0.15 pT. The current distribution in the plane with $z = -4$ is reconstructed using (2). The results are shown in Fig. 4.

C. Generation of External Noise Fields

External noise fields are generated assuming two magnetic dipoles outside the spherical conductor. One magnetic dipole is located at $(-20, -30, 215)$ with a dipole moment equal to $(0, 0, D_1)$, and the other magnetic dipole is located at $(-100, -5, 5)$ with a moment equal to $(D_2, 0, 0)$. The two components, D_1 and D_2 , are assumed to randomly fluctuate at each sampled time t_k , and are assumed not to be correlated

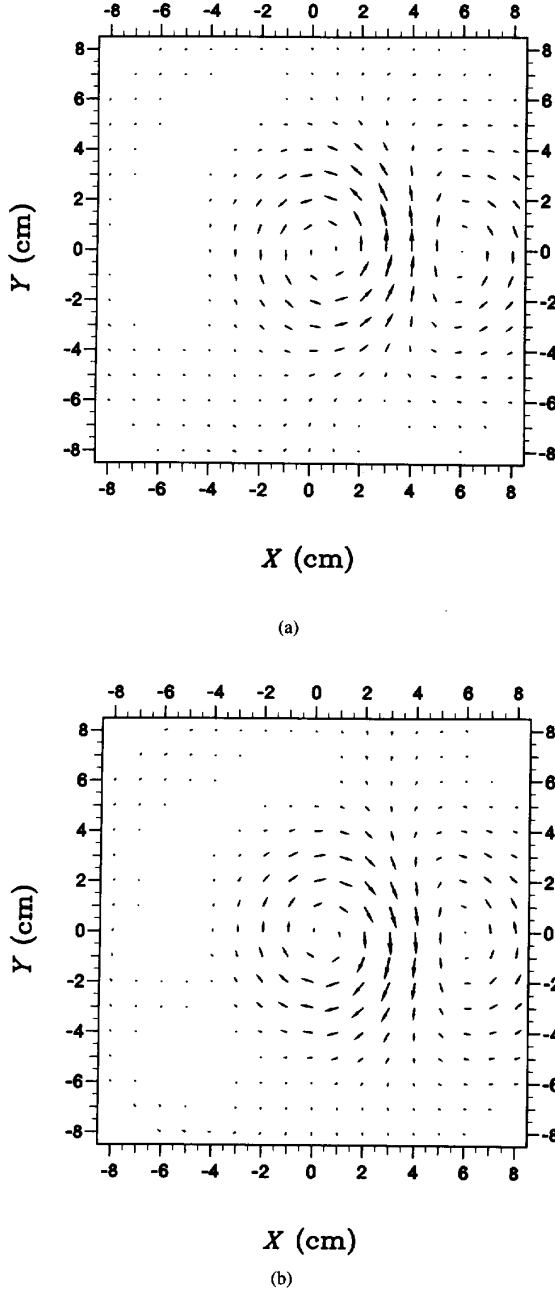


Fig. 4. Results of conventional reconstruction of a simulated evoked neural source. Results are obtained using simulated evoked field data at $t = t_e$ and $t = t_f$, i.e., using (a) $S_m(t_e)$ and (b) $S_m(t_f)$. The plane $z = -4$ is reconstructed using (2).

to each other. The average values, $\langle D_1 \rangle$ and $\langle D_2 \rangle$, are set at zero and the standard deviations, $\sqrt{\langle (D_1)^2 \rangle}$ and $\sqrt{\langle (D_2)^2 \rangle}$, are set at 1.2 mAm^2 and 0.08 mAm^2 , respectively.

The external noise data measured at the m th detector channel at time t_k caused by two magnetic dipoles are defined as $E_m(t_k)$. This is calculated by subtracting the output of the gradiometer's upper coil from that of the lower coil.

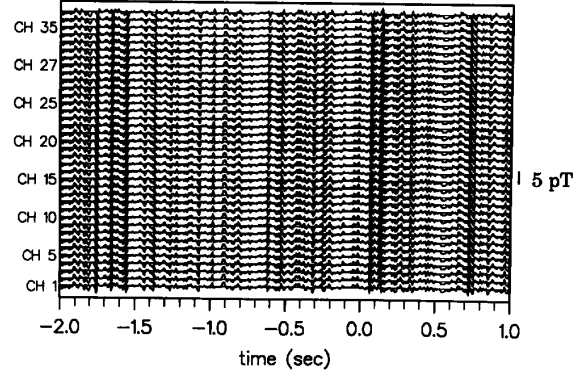


Fig. 5. Thirty-seven channel recordings of simulated external noise data $E_m(t_k)$. The data are calculated assuming that two randomly fluctuating magnetic dipoles exist outside the spherical conductor.

The calculated results of this $E_m(t_k)$ for $-2 \leq t \leq 1$ are shown in Fig. 5. The intensity of the external field is evaluated by calculating $\sqrt{\frac{1}{KM} \sum_{k=1}^K \sum_{m=1}^M E_m^2(t_k)}$. This value is 0.98 pT in this case. The external noise data $E_m(t_k)$ are added to the simulated evoked field data $S_m(t_k)$. In order to check the influence of these external noise fields, the evoked ECD is conventionally reconstructed with (2) using the two data sets, $E_m(t_e) + S_m(t_e)$ and $E_m(t_f) + S_m(t_f)$. Here, the ratios, $\sqrt{\sum_{m=1}^M E_m^2(t_e) / \sum_{m=1}^M S_m^2(t_e)}$ and $\sqrt{\sum_{m=1}^M E_m^2(t_f) / \sum_{m=1}^M S_m^2(t_f)}$ are 1.5 and 11.2 , respectively. The reconstruction results are shown in Figs. 6(a) and (b). Comparing Fig. 6 with Fig. 4, it can be seen that the reconstructed results are greatly distorted due to the existence of large external noise fields.

D. Generation of Simulated Brain Noise

Next, the noise caused by spontaneous brain activity is simulated. Here, the model of the source is a current dipole rotating in the x - z plane with a random phase; the dipole exists at a fixed point inside the spherical homogeneous conductor. The dipole is assumed to be located at $(-5, -1, -5)$. The moment of this noise dipole, $\mathbf{q} = (q_x(t_k), q_y(t_k), q_z(t_k))$, is assumed to be

$$q_x(t_k) = |\mathbf{q}| \cos(\theta_{k-1} + \Delta\theta_k)$$

$$q_y(t_k) = 0, \quad q_z(t_k) = |\mathbf{q}| \sin(\theta_{k-1} + \Delta\theta_k).$$

Here, θ_{k-1} is the phase of the rotation at t_{k-1} , and $\Delta\theta_k$ is the phase difference between t_{k-1} and t_k . This $\Delta\theta_k$ is determined by generating a uniform random number whose range is $0 \leq \Delta\theta_k \leq \pi/2$. The intensity of the noise-dipole moment, $|\mathbf{q}|$, is set at $0.05 \text{ mA}\cdot\text{mm}$.

This simulated brain noise measured by the m th detector channel at t_k is defined as $\Lambda_m(t_k)$. The calculated results of $\Lambda_m(t_k)$ for $-2 \leq t_k \leq 1$ are shown in Fig. 7. The average noise intensity $\sqrt{\frac{1}{KM} \sum_{k=1}^K \sum_{m=1}^M \Lambda_m^2(t_k)}$ is 0.21 pT in this case. In order to check the influence of this brain noise, a conventional reconstruction of the evoked ECD employing (2) is

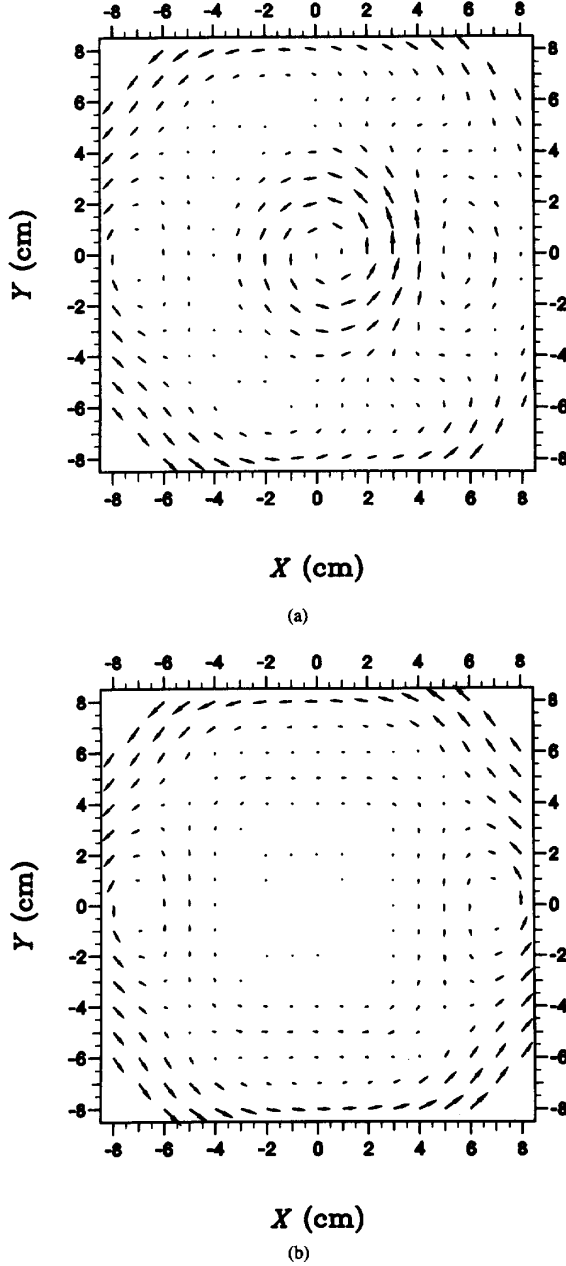


Fig. 6. Results of conventional reconstruction of a simulated evoked neural source. Results are obtained using evoked field data overlapped by simulated external noise field data, i.e., using (a) $S_m(t_e) + E_m(t_e)$ and (b) $S_m(t_f) + E_m(t_f)$. The plane $z = -4$ is reconstructed using (2).

performed using two data sets, $S_m(t_e) + \Lambda_m(t_e)$ and $S_m(t_f) + \Lambda_m(t_f)$. Here, the ratios, $\sqrt{\sum_{m=1}^M \Lambda_m^2(t_e) / \sum_{m=1}^M S_m^2(t_e)}$ and $\sqrt{\sum_{m=1}^M \Lambda_m^2(t_f) / \sum_{m=1}^M S_m^2(t_f)}$, are 1.6 and 0.83, respectively. The reconstruction results are shown in Figs. 8(a) and (b). A comparison with the reconstruction shown in Fig. 4 shows that considerable distortions caused by the simulated brain noise exist in Figs. 8(a) and (b).

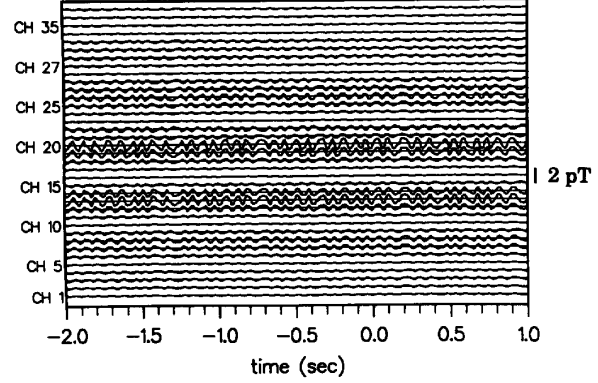


Fig. 7. Thirty-seven channel recordings of simulated brain noise data $\Lambda_m(t_k)$. The data are calculated assuming that one randomly rotating current dipole exists at $(-5, -1, -5)$ inside the spherical conductor.

E. Reduction of Noise Field Influence

The evoked field data influenced by both the noise magnetic dipole field and the simulated brain noise field, $B_m(t_k)$, are calculated by $B_m(t_k) = S_m(t_k) + E_m(t_k) + \Lambda_m(t_k)$. First, the reconstruction with the Moore-Penrose generalized inverse, i.e. with (2), is performed using the two data sets, $B_m(t_e)$ and $B_m(t_f)$. The reconstructed results are shown in Figs. 9(a) and (b). The results contain large distortions.

Then, the noise covariance matrix is calculated using a portion of the data $B_m(t_k)$ before stimulus application, i.e. using $B_m(t_k)$ with $-2 \leq t_k < 0$. The total number of data sampling points contained in this time interval is denoted by K_c . In this computer simulation, K_c is equal to 200. Assuming that the external noise has an ergodic property, the (i, j) element of the noise covariance matrix C_{ij} can be calculated using

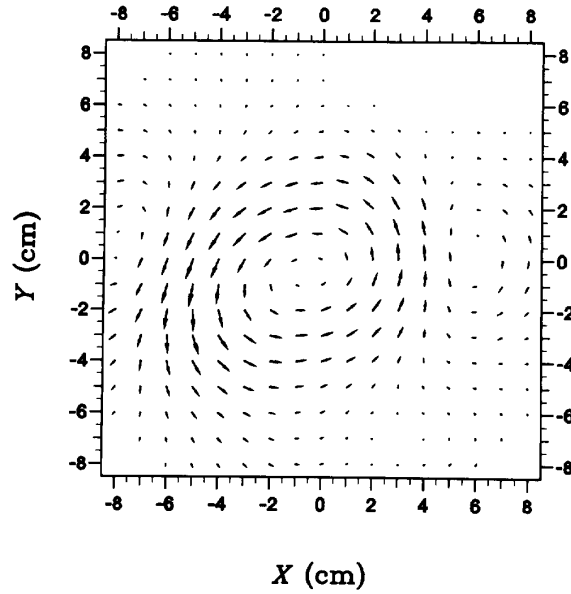
$$C_{ij} = \frac{1}{K_c} \sum_{k=1}^{K_c} (B_i(t_k) - \frac{1}{K_c} \sum_{k=1}^{K_c} B_i(t_k)) (B_j(t_k) - \frac{1}{K_c} \sum_{k=1}^{K_c} B_j(t_k)). \quad (8)$$

The two data sets, $B_m(t_e)$ and $B_m(t_f)$, are reconstructed using the proposed reconstruction, namely (5), with the noise covariance matrix obtained using (8). The results are shown in Figs. 10(a) and (b).

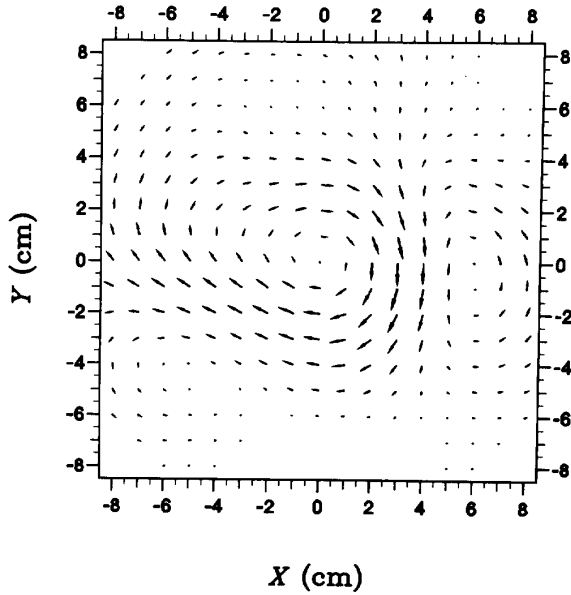
By comparing Fig. 4 with Fig. 10, it is clear that the influence of the external noise field is almost completely removed in the results shown in Fig. 10. Conversely, in Fig. 9, the external noise field greatly influences the reconstructed results, so the conventional method gives almost meaningless results. A comparison of Figs. 9 and 10 clearly demonstrates the effectiveness of the proposed reconstruction.

IV. CONCLUSION

This paper proposes a new method of reconstructing current-density distributions from biomagnetic measurement. It can reduce the influence of external noise fields by incorporating their spatial coherence. Experiments using computer gener-



(a)

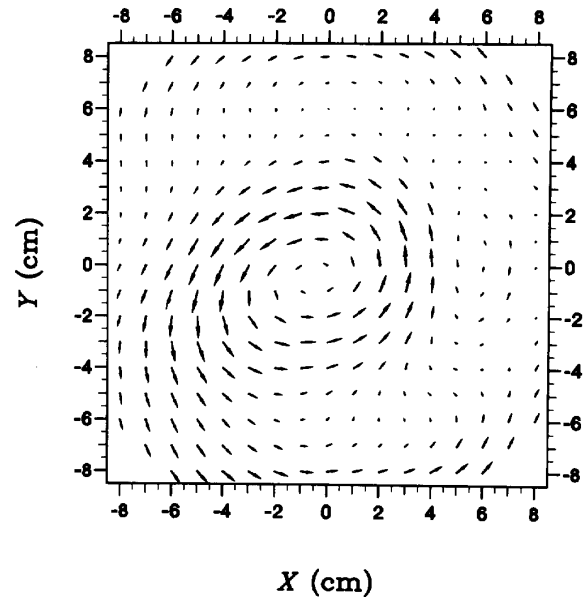


(b)

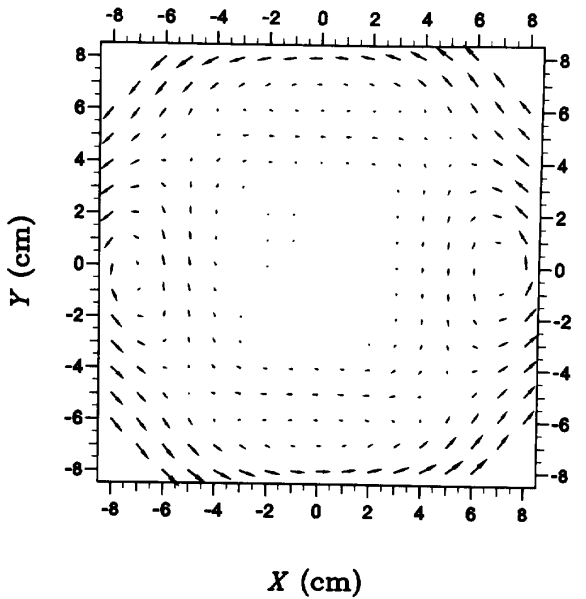
Fig. 8. Results of conventional reconstruction of a simulated evoked neural source. Results are obtained using evoked field data overlapped by simulated brain noise field data, i.e. using (a) $S_m(t_e) + \Lambda_m(t_e)$ and (b) $S_m(t_f) + \Lambda_m(t_f)$. The plane $z = -4$ is reconstructed using (2).

ated noise fields demonstrate that the method can reconstruct current distributions from data severely affected by external noise.

The proposed reconstruction method is useful for cases where the measurements must be conducted without a magnetically shielded room or with an inexpensive low-quality shielded room. More interesting cases to which the proposed method is applicable are cases where the signal fields overlap



(a)



(b)

Fig. 9. Results of conventional reconstruction of a simulated evoked neural source. Results are obtained using evoked field data overlapped by both simulated external noise data and simulated brain noise data, i.e., using (a) $S_m(t_e) + E_m(t_e) + \Lambda_m(t_e)$ and (b) $S_m(t_f) + E_m(t_f) + \Lambda_m(t_f)$. The plane $z = -4$ is reconstructed using (2).

with noise fields of biological origin. The possibility of this application is demonstrated in Section 3, which simulates a situation where the magnetic field caused by spontaneous brain activity overlaps the evoked neuromagnetic field.

When the noise source is located very close to the signal source and when the dipole moment of the noise source is very similar to that of the signal source, the covariance matrix

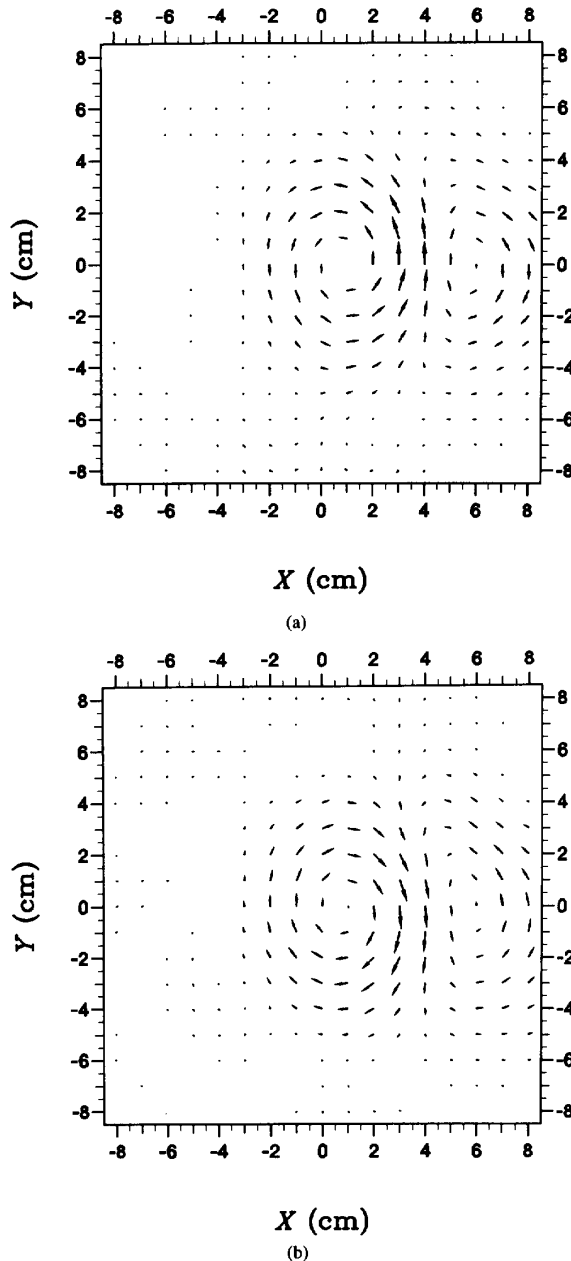


Fig. 10. Results of proposed reconstruction of a simulated evoked neural source. Results are obtained using evoked field data overlapped by both simulated external noise and simulated brain noise data, i.e., using (a) $S_m(t_e) + E_m(t_e) + \Lambda_m(t_e)$ and (b) $S_m(t_f) + E_m(t_f) + \Lambda_m(t_f)$. The plane $z = -4$ is reconstructed using (5), with the noise covariance matrix obtained using (8).

of the signal can be very similar to the noise covariance matrix. In such cases, the proposed method obviously removes signal information as well as external noise influence. Such situations may occur in brain noise cases. This limit on the method's effectiveness is currently under investigation, and a recently proposed evaluation method will be helpful for this investigation [15].

The method's effectiveness in actual applications may also be limited if the noise statistical properties are not time invariant. Generally, the statistical properties of noise caused by spontaneous brain activity cannot be considered time invariant. However, the statistical properties of such noise can be assumed to be nearly stationary if the time window for calculating the covariance matrix is close to the portion of data used for current density reconstruction. An experiment that suggests the validity of this assumption for pathological rhythmic slow wave from an epileptic patient has very recently been reported [16]. Since very little is known about the behavior of brain-noise source, the model used to express the brain noise source in our computer experiments is chosen mainly out of convenience. Thus, the method's effectiveness in removing brain noise influence must ultimately be evaluated through a large number of applications using actually measured data.

Finally, it should be mentioned that the spatial filter algorithm recently proposed by Robinson et al. [17] can also provide distributed current source reconstruction in the presence of external noise disturbances. Although this algorithm is not explained in detail [17], a comparison between Robinson's method and the method proposed in this paper should be performed at a future date.

REFERENCES

- [1] S. J. Williamson and L. Kaufman, "Biomagnetism," *J. Magnetism and Magnetic Mater.*, vol. 22, pp. 129–201, 1981.
- [2] K. Sekihara, H. Haneishi, and N. Ohya, "Parameter estimation of multiple biomagnetic current dipoles using simulated annealing," in *Proc. SPIE Conf. on Digital Image Synthesis and Inverse Optics* vol. 1351, pp. 410–416, 1990.
- [3] M. S. Hämäläinen and R. J. Ilmoniemi, "Interpreting measured magnetic fields of the brain: Estimates of current distributions," *Report TKK-F-A559*, Helsinki University of Technology, Helsinki, Finland, 1984.
- [4] J. Z. Wang, S. J. Williamson, and L. Kaufman, "Magnetic source images determined by a lead-field analysis: The unique minimum-norm least-squares estimation," *IEEE Trans. Biomed. Eng.*, vol. 39, pp. 565–75, 1992.
- [5] R. Graumann, "The reconstruction of current densities," *Helsinki University of Technology, Report on Biomagnetic Localization and 3D Modelling*, TKK-F-A689, Helsinki University, Helsinki, Finland, pp. 172–186, 1991.
- [6] J. Knuutila and M. S. Hämäläinen, "Characterization of brain noise using a high sensitivity 7-channel magnetometer," in *Proc. Sixth Internat. Conf. Biomagnet.*, pp. 186–189, 1987.
- [7] K. Sekihara, Y. Ogura, and M. Hotta, "Maximum likelihood estimation of current dipole parameters for data obtained using multichannel magnetometer," *IEEE Trans. Biomed. Eng.*, vol. 39, pp. 558–62, 1992.
- [8] J. Vrba, J. McCubbin, S. Lee, A. A. Fife, and M. B. Burbank, "Noise cancellation in biomagnetometers," in *Proc. Seventh Internat. Conf. Biomagnet.*, pp. 733–736, 1989.
- [9] J. Sarvas, "Basic mathematical and electromagnetic concepts of the biomagnetic inverse problem," *Phys. Med. Biol.*, vol. 32, pp. 11–22, 1987.
- [10] C. L. Lawson and R. J. Hanson, *Solving Least Squares Problems*. Englewood Cliffs, NJ: Prentice-Hall, Inc., 1974.
- [11] C. W. Groetsch, *The Theory of Tikhonov Regularization for Fredholm Equations of The First Kind*. London, UK: Pitman, 1984.
- [12] H. C. Andrews and B. R. Hunt, *Digital Image Restoration*. Englewood Cliffs, NJ: Prentice-Hall, Inc., 1977.
- [13] W. K. Pratt, *Digital Image Processing*. John Wiley & Sons, New York, 1978.
- [14] S. F. Gull and G. J. Daniell, "Image reconstruction from incomplete and noisy data," *Nature*, vol. 272, pp. 686–70, 1978.
- [15] K. Abraham-Fuchs and K. Sekihara, "Effect of biomagnetic signal processing on source localization estimated by means of statistical source distributions," in *Proc. 14th Annu. Int. Conf. IEEE Eng. in Medicine and Biology Soc.*, pp. 1768–1769, 1992.

- [16] K. Abraham-Fuchs, K. Sekihara, H. Stefan and E. Hellstrand, "Separation of epileptic spike activity from background rhythmic brain activity using noise spatial coherence," *Proceedings of the 14th annual international conference of IEEE Engineering in Medicine and Biology Society, Satellite Symp. Neurosci. and Technol.*, pp. 8-14, 1992.
- [17] S. B. Robinson and D. F. Rose, "Current source image estimation by spatially filtered MEG," in M. Hoke et al., Eds., *Biomagnetism: Clinical Aspects*, New York: Elsevier Publishers, 1992, pp. 761-764.